

Accepted Manuscript

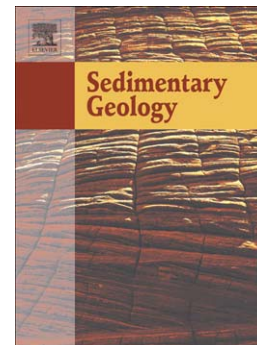
Were fossil spring-associated carbonates near Zaca Lake, Santa Barbara, California deposited under an ambient or thermal regime?

Yadira Ibarra, Frank A. Corsetti, Michael I. Cheetham, Sarah J. Feakins

PII: S0037-0738(13)00229-7
DOI: doi: [10.1016/j.sedgeo.2013.12.005](https://doi.org/10.1016/j.sedgeo.2013.12.005)
Reference: SEDGEO 4711

To appear in: *Sedimentary Geology*

Received date: 13 October 2013
Revised date: 22 December 2013
Accepted date: 23 December 2013



Please cite this article as: Ibarra, Yadira, Corsetti, Frank A., Cheetham, Michael I., Feakins, Sarah J., Were fossil spring-associated carbonates near Zaca Lake, Santa Barbara, California deposited under an ambient or thermal regime?, *Sedimentary Geology* (2014), doi: [10.1016/j.sedgeo.2013.12.005](https://doi.org/10.1016/j.sedgeo.2013.12.005)

This is a PDF file of an unedited manuscript that has been accepted for publication. As a service to our customers we are providing this early version of the manuscript. The manuscript will undergo copyediting, typesetting, and review of the resulting proof before it is published in its final form. Please note that during the production process errors may be discovered which could affect the content, and all legal disclaimers that apply to the journal pertain.

Were fossil spring-associated carbonates near Zaca Lake, Santa Barbara, California deposited under an ambient or thermal regime?

Yadira Ibarra ^{a,*}, Frank A. Corsetti ^a, Michael I. Cheetham ^a, Sarah J. Feakins ^a

^a University of Southern California, Department of Earth Sciences, Los Angeles, CA 90089 USA

*Corresponding author

E-mail address: yibarra@usc.edu

Telephone number: 1-213-740-7653

Fax number: 1-213-740-8801

Address: ZHS 117, 3651 Trousdale Parkway

Los Angeles, CA, USA 90089-0740

ABSTRACT

A previously undescribed succession of currently-inactive spring-associated carbonates located near Zaca Lake, Southern California, was investigated in order to determine the nature of deposition (ambient temperature or hydrothermal water, as both are found within the region). The carbonate deposits are up to ~1 m thick and formed discontinuously for over 200 m in a narrow valley between two ridges that drain Miocene Monterey Formation bedrock. Depositional facies along the presently dry fluvial path include barrage deposits, narrow fluvial channels, and cascade deposits. The carbonates are mesoscopically banded and contain ubiquitous micro- to macrophyte calcite encrusted fabrics. All of the depositional facies contain alternating bands (~.05 mm to 5 mm thick) of dark brown and light brown isopachous calcite; the dark brown bands are composed of dense isopachous bladed calcite, whereas the light brown bands are composed of bundles of calcite tubules interpreted as the biosignature of the desmid microalgae *Oocardium stratum*. Oxygen isotope thermometry utilizing modern water $\delta^{18}\text{O}$ values from the piped spring reveal depositional water temperature estimates that collectively range from ~11–16 °C. Stable isotope carbon values exhibit a mean $\delta^{13}\text{C}$ value of $-9.01 \pm 0.62\text{‰}$ (1 σ , $n=27$). Our petrographic and geochemical data demonstrate that (1) inactive carbonates were likely sourced from ambient temperature water with a strong soil-zone $\delta^{13}\text{C}$ signal, (2) the *Oocardium* calcite biosignature can be used to infer depositional temperature and flow conditions, and (3) the occurrence of extensive carbonates (especially the presence of a perched cascade deposit) indicate the carbonates formed when conditions were much wetter.

Key Words: *Oocardium stratum*; tufa; travertine; carbonate springs; biosignatures

1. Introduction

Terrestrial carbonates that form via spring activity are sensitive to the environment in

which they form, potentially serving as valuable archives of hydrology, water chemistry, biology and climate of their local depositional setting (Chafetz et al., 1991; Fouke et al., 2000; Pentecost, 2005; Andrews, 2006; Cremaschi et al., 2010; Sanders et al., 2011). Spring-associated carbonate deposits are commonly classified based on the temperature and origin of the carrier CO₂ of the water from which they are sourced (e.g., Ford and Pedley, 1996). The term *travertine* refers to carbonate deposits that form from high-temperature spring water, where the CO₂ is sourced from hydrothermal fluids, whereas the term *tufa* has been assigned to ambient temperature carbonate spring precipitates, where the CO₂ is sourced from local soils and the atmosphere (Ford and Pedley, 1996). Their distinct hydrologic origins thereby provide different information on the environmental setting of deposits that are no longer active. The presence of travertine, for example, has implications for nearby hydrothermal/volcanic activity (Hancock et al., 1999; Fouke et al., 2000), whereas the groundwater-fed nature of tufa deposits results in a strong influence by local climate (Andrews, 2006).

In order to accurately interpret depositional information from a given fossil/inactive terrestrial carbonate succession, we must first determine the hydrological regime under which the carbonates formed (ambient temperature, thermal, or a mix of thermal and ambient water). Degree of lithification, macrophyte encrustations, and organic carbon content allow travertine to be distinguished from tufa (Ford and Pedley, 1996; Minissale et al., 2002; Gandin and Capezzuoli, 2008; Capezzuoli et al., *Accepted article*). However, poor textural preservation, similar sedimentological facies, and interlayering/mixing of tufa and travertine in sites where (1) hydrothermally sourced waters cool with extensive lateral transport and/or (2) where thermal and ambient waters from the same site mix to produce interlayering facies of travertine and tufa (e.g., Capezzuoli et al., 2008; Pedley, 2009) may complicate our ability to fully decipher depositional

information from fossil/inactive deposits. For these reasons, geochemical analyses (e.g., stable isotopes) are often used to infer the hydrologic nature of inactive spring carbonates (Gonfiantini et al., 1968; Szulc and Cwizewicz, 1989; Guo et al., 1996; Minissale et al., 2002; Andrews and Brasier, 2005; Kele et al., 2008). Nonetheless, terrestrial carbonates are highly susceptible to recrystallization, possibly compromising geochemical signatures and thus primary structures are desirable.

A potential complimentary approach to verify the hydrology of deposition is to examine the micromorphology of the deposit. It is well-established that microorganisms can contribute to the formation and alteration of terrestrial spring carbonates (Freytet and Verrecchia, 1998; Riding, 2000; Golubić et al., 2008; Pedley, 2009; Arp et al., 2010; Manzo et al., 2012). Much of the focus on terrestrial carbonates has been on the interplay between the physicochemical and biological mechanisms that contribute to carbonate precipitation. Active carbonate-depositing springs serve as natural laboratories where we can study the extent to which microorganisms might influence the precipitation of carbonates and other minerals. By examining mineral phases/structures associated with specific taxa (e.g., Freytet and Plet, 1996; Freytet and Verrecchia, 1998), we may be able to constrain environmental signals from dormant/inactive deposits presuming they have not yet become diagenetically altered beyond recognition. Here we combine a multiscale facies approach (*sensu* Shapiro, 2000) with analyses of stable isotopes to determine the depositional regime (ambient or thermal) of previously undescribed fossil/inactive spring carbonates located in Santa Barbara County, Southern California as both cold springs and hot springs have been reported in the surrounding area (USGS, 1995).

2. Geological and environmental context of study site

Spring-derived carbonate deposits are located about 2 km upstream of Zaca Lake in Santa Barbara County, California, USA (Fig. 1). In 1911 a natural spring was boxed and piped to provide water for consumption (Fig. 1B) such that carbonate deposition downstream has not been observed in the modern. Carbonates crop out discontinuously for over 200 m along the stream grade bed of a narrow valley that is bound by two ridges composed of the carbonate-rich Miocene Monterey Formation (Hall, 1981). The ridges define the relatively small catchment that drains into Zaca Lake, one of only a few naturally-occurring lakes in Southern California.

Two distinct units of spring-related carbonate growth have been observed. The first spring carbonate succession, the focus of the majority of the work described here, was deposited discontinuously for approximately 200 m along the stream grade bed of the valley (Fig. 1B). The width of the spring carbonate transect varies from about 1 m to approximately the width of the valley floor (~15 m) and ranges in thickness from 0 to about 1 m. A second carbonate unit (approximately 15 m in lateral extent and ~2 m thick) occurs perched upon the slope of the north ridge about 10 m above the modern stream grade bed (Fig. 1B). The ages of the carbonate units are unknown, but we assume a relatively young age (possibly late Quaternary) based on the geomorphic position of the deposits within the valley system.

3. Methods

3.1 Facies descriptions

In our approach, we describe the macro- to micro- characteristics (*sensu* Shapiro, 2000) of four distinct facies (Fig. 1B) along the spring carbonate transects. Carbonate rock samples were obtained from the topmost (~10–20 cm) part of the four sections where there was good surface exposure and samples were easily accessible. Samples were slabbed, polished, and scanned for mesostructural studies (cm scale). Microstructural observations were carried out via

light microscopy of thin sections. Complementary thin-section rock pieces were etched with diluted HCl and examined further using a scanning electron microscope (SEM). Mineralogy was determined via X-ray diffraction (XRD) at the Los Angeles Museum of Natural History. Here, we focus on the microfabric of a particular lamination that is conspicuous in outcrop and hand sample.

3.2 Carbonate isotopic analyses

Isotopic analyses of carbonate oxygen and carbon were conducted on an Elementar Americas Inc. (Micromass Ltd) Isoprime stable isotope ratio mass spectrometer (IRMS) with a multi-prep/carbonate device and dual inlet at the Stott Laboratory at the University of Southern California. Samples were drilled from polished hand sample specimens after careful inspection for recrystallization via thin section analyses. Samples are measured relative to CO₂ reference gas calibrated against the NBS-19 ($\delta^{18}\text{O}$ value +2.20‰, $\delta^{13}\text{C}$ value +1.95‰) carbonate standard, which allows for normalization to the 2-point VPDB-LVSEC isotopic scale. The precision of this determination is better than 0.06‰ and 0.04‰ (1 σ , $n = 20$) for $\delta^{18}\text{O}$ and $\delta^{13}\text{C}$, respectively. A working standard (carbonate, $\delta^{18}\text{O} -1.88\text{‰}$, $\delta^{13}\text{C}$ value +2.07‰) monitors precision during the course of the run to 0.06‰ and 0.04‰ (1 σ , $n = 43$) for $\delta^{18}\text{O}$ and $\delta^{13}\text{C}$, respectively.

3.3 Water isotope analyses

Modern water samples from the spring were analyzed for $^{18}\text{O}/^{16}\text{O}$ and D/H ratios using a spectroscopic Liquid-Water Isotope Analyzer (Los Gatos Research, Inc) at the University of California at Davis or cavity ring-down spectroscopy (Picarro Inc.) at the SIRFER laboratory at the University of Utah for isotopic determination of $\delta^{18}\text{O}$ and δD . Samples are calibrated against working standards of known isotopic composition, which allow for normalization to the 2-point Vienna Standard Mean Ocean Water (VSMOW, 0 ‰) and Standard Light Antarctic Precipitation

(SLAP, $\delta^{18}\text{O}$ value -55.5‰ , δD value -428‰) isotopic scale. The precision of replicate injections (1 σ) of these standards was better than 0.2‰ and 2‰ for $\delta^{18}\text{O}$ and δD , respectively.

4. Results

4.1 Facies descriptions

We targeted four of the most prominent carbonate exposures along the fluvial path (all labeled in Fig. 1B and pictured in Fig. 2): (1) perched cascade ($34^{\circ}46'20''\text{N}$, $120^{\circ}02'216''\text{W}$), (2) fluvial barrage ($34^{\circ}46'43''\text{N}$, $120^{\circ}01'219''\text{W}$), (3) fluvial channel ($34^{\circ}46'040''\text{N}$, $120^{\circ}01'281''\text{W}$), and (4) fluvial cascade ($34^{\circ}46'601''\text{N}$, $120^{\circ}01'392''\text{W}$). The perched deposit is a succession of carbonates that formed on a steep slope laterally adjacent to the boxed spring but about 10 m above the present valley floor (Fig. 1B). Carbonates are about 15 m in lateral extent and up to 2 m thick. The unit terminates with a cascade facies (Fig. 2A) that contains overhanging carbonate curtains (*sensu* Pedley, 1990). The carbonate samples investigated in this study originate from the outermost face of the cascade wall (Fig. 2A).

The barrage carbonates (*sensu* Pedley, 1990) are the first extensive carbonates (~ 20 m lateral extent) that formed on the valley floor about 60 m downslope and about 5-10 m lower in altitude from the boxed spring. Carbonates crop out and occupy a width of about 15 m along the valley floor and are less than 0.5 m thick (Fig. 2B). Although most of the carbonate surface is covered in dense mosses and foliage (Fig. 2B), some laminated structures can be seen in outcrop, as well as molds of encrusted leaves and plant debris. Samples analyzed from the barrage facies originate from the top 20 cm of small dams.

The next prominent carbonate facies is a fluvial channel that occurs about 90 meters down slope of the boxed spring on the north side of the valley (Fig. 2C). The channel is about 2 m wide and about 1 m thick and exhibits successive draping carbonate fabrics. Presently, the

carbonate surface is covered in thin colonies of dry mosses. Erosive features are common below the channel where fast flowing water could have scoured and transported carbonate downstream. Also, successive carbonate drapes could indicate the deposit underwent periods of non-deposition and possibly erosion. Carbonate samples examined from this deposit originate from the outermost surface of the terrace face (~20 cm-thick).

The distal end of the fluvial carbonate transect (~about 180 m from the boxed spring) terminates with a cascade deposit that is about 15 m wide and contains a drop in elevation of about 10 m from the top to the bottom of the cascade (Fig. 2D). Within the fluvial cascade, at least two distinct episodes of carbonate growth can be observed on the surface of the deposit: (1) a basal white to light brown deposit widely distributed on the cascade face and (2) a brown, highly porous carbonate with a patchy distribution, typically restricted to small (~10 cm wide and ~5 cm thick) dams that drape the basal white deposit. The total thickness of the cascade carbonate is about 0.5 m. The carbonate samples examined from this deposit originate from the basal white to light brown carbonates and were collected near the top of the cascade (upper ~20 cm).

All of the carbonate facies examined contain carbonate pieces that are not attached to the deposit potentially indicating they were transported from up the valley. In particular, large (m-scale) talus blocks eroded from the perched cascade and lie unconformably along the valley channel.

4.2 Mesostructure

Representative polished rock samples from the four facies are pictured in Fig. 3. Mesoscopically, the samples contain bands of variable thicknesses that range from about 1mm to 5 mm. Polished samples from the perched deposit are largely composed of dense light and dark

bands. In cross section, the barrage deposits, fluvial channel, and fluvial cascade samples all contain abundant macro- and microphyte molds (Fig. 3C). Additionally, there is considerable intra- and inter-fabric variability among the different facies, despite all having been collected from the top ~10–20 cm surfaces of each deposit. While the internal structure and thicknesses of bands varies across the different deposits, a prominent similarity is the occurrence of conspicuous light brown bands (~3 mm to 5 mm thick; see arrows in Fig. 3) that form a marked contrast with the dominant dark brown color of other fabrics. The bands are composed of isopachous fibrous calcite crystals (Fig. 4). In some cases, the calcite grew radially, likely around twigs or other debris that were deposited in the spring system. Its fibrous nature is better observed in a freshly broken piece (Fig. 4A). Light brown and dark, dense bands commonly alternate with one another and are both composed of calcite (Fig. 4B).

4.3 Microstructure observations of light brown and dark brown bands

In contrast to the polished hand samples, the dark, dense bands appear lighter in color in transmitted light and the light brown fibrous bands appear darker (contrast Fig. 4B with Figs. 4C-E). The dark, dense bands are composed of isopachous bladed calcite crystals with well-developed pyramidal terminations (Fig. 4D), whereas the light brown bands are composed of bundles of calcite tubules (Fig. 5E). The tubules bifurcate along their length to form fan-shaped bundles (Figs. 5A-B). Each fan-shaped tubule bundle is approximately 1.5 mm in length and averages about 0.5 mm in thickness (see outline of a fan-shaped tubule bundle in Fig. 5A). An oblique SEM view of the bottom of several tubule bundles displays that each bundle originated from a common point (Fig. 5C). Figs. 5D-E illustrate the initially hollow nature of the tubules.

The tubules have a consistent diameter in vertical cross section ($20 \pm 2 \mu\text{m}$). The consistent diameter of the tubules is further confirmed via a horizontal cross-section of a tubule

bundle (Figs. 5F-G). Under cross-polarized light, the tubule walls in a given bundle exhibit unit extinction (Fig. 5B) indicating each bundle of tubules is a monocrystal.

4.4 Carbonate isotopic analyses

The oxygen and carbon isotopic values of micro-drilled carbonate samples are listed in Table 1, differentiating their fabric type: light brown bands (LBB) and dark brown bands (DBB). Samples marked with an asterisk in Table 1 indicate the mean $\delta^{18}\text{O}$ and $\delta^{13}\text{C}$ values of at least three measurements along the respective sample band. The standard deviation (1 σ) along a single band is less than 0.70‰ and 0.20‰ for $\delta^{13}\text{C}$ and $\delta^{18}\text{O}$, respectively.

The $\delta^{18}\text{O}$ values of the LBB from all four depositional facies range from -6.78‰ to -7.48‰ with a mean value of $-7.12 \pm 0.20\text{‰}$ (1 σ , $n = 14$). The DBB exhibit $\delta^{18}\text{O}$ values that range from -6.77 to -7.66‰ with a mean value of $-7.27 \pm 0.28\text{‰}$ (1 σ , $n = 13$). The mean $\delta^{13}\text{C}$ value for the LBB is $-8.92 \pm 0.65\text{‰}$ (1 σ , $n = 14$) and the DBB exhibit a mean $\delta^{13}\text{C}$ value of $-9.17 \pm 0.37\text{‰}$ (1 σ , $n = 13$).

4.5 Water isotopic analyses

Water samples from the boxed spring were sampled eight times between 2009 and 2012. Measured $\delta^{18}\text{O}$ and δD values are listed in Table 2 with their corresponding collection date. The isotopic composition of modern spring water is relatively constant with a mean $\delta^{18}\text{O}$ value of $-7.58 \pm 0.23\text{‰}$ (1 σ , $n = 8$) and δD value of $-46.7 \pm 2.3\text{‰}$ (1 σ , $n = 8$). Paired $\delta^{18}\text{O}$ and δD values place the modern spring water as slightly enriched above the global meteoric water line.

5. Discussion

5.1 *Oocardium stratum calcite biosignature*

The fan-shaped tubular crystal structure composed of 20 μm diameter bifurcating tubules is strikingly similar to the unique calcite microstructure formed in the presence of the desmid

microalgae *Oocardium stratum* (Nägeli, 1849). *Oocardium* is a colonial desmid whose cell diameter ranges from 17–20 μm and is known to live in colonies of about 100 cells (Pentecost, 1991). Individual cells release copious amounts of mucilage preferentially on one end of the cell. Calcite nucleates on and around the mucilage portion and as the cell divides, the calcite takes the shape of the secreted mucilage tube. Continued cell division results in a monocrystal fan-shape bundle composed of bifurcating calcite tubules, see Golubić et al. (1993) and Sanders and Rott (2009) for growth illustrations. Live cells remain above the calcite rim via continuous secretion of mucilage, which is believed to help elevate the cell (Golubić et al., 1993). Former calcite colonies of *Oocardium* calcite (labeled ‘c’ in Fig. 6A) can be identified in thin section based on the presence of the tubules, their consistent diameter, bifurcation pattern, and unit extinction pattern of the tubule walls in cross-polarized light highlighting a monocrystal (Fig. 5B). The boundary of individual fan-shaped bundles is well-defined in thin section (Figs. 6B-C). A horizontally and vertically oriented boundary between two fans displays the empty tubules that likely once enclosed an *Oocardium* cell (Fig. 6D).

5.2 Environmental conditions associated with Oocardium calcite deposition

Oocardium stratum is known as an unusual desmid for the way it becomes encrusted in calcite and for being endemic to freshwater carbonate depositing sites (Wallner, 1933; Pentecost, 1991). In sites that contain extensive active *Oocardium* colonies, a water temperature range of ~9–13 °C is frequently reported (Rott et al., 2009; Sanders and Rott, 2009; Gesierich and Kofler, 2010; Linhart, 2011), suggesting the Zaca carbonate fabrics were sourced from cold water rather than thermal waters. *Oocardium* is known to exist in slightly warmer or colder conditions (Pentecost, 1991; Golubić et al., 1993; Gradzinski, 2010); however its growth was not observed throughout the year and the possibility of water temperature controlling its development and

persistence was not directly addressed. Linhart (2011) noted that optimal growth conditions for *Oocardium* appeared at a water temperature of 13 °C based on a 17 month study on actively growing *Oocardium* colonies that were monitored on a weekly basis.

Another common growth element of *Oocardium stratum* is its preference for swiftly to fast flowing water (Mathews et al., 1965; Pentecost, 1991). Although Gradzinski (2010) reports growth under ‘sluggish flow’, growth in water that accumulates in pool facies has not previously been observed. This characteristic is consistent with reports of *Oocardium* typically occurring in association with cascade/waterfall facies (Pfiester, 1976; Golubić et al., 1993; Pentecost and Zhang, 2000; Rott et al., 2009), i.e., areas that when wet will always experience flow. The samples for this study were collected from the cascade facies, further corroborating our interpretation of the structures. The occurrence of *Oocardium* in the barrage facies indicate they could have formed during an episode of very fast flow accumulating at the edges of small dams, where our samples originate from. Given the intimate relationship between *Oocardium* and calcite deposition, it is reasonable that *Oocardium* colonies would prefer to colonize sites that degas CO₂ quickly and consequently favor rapid carbonate deposition.

Considering the spring was boxed in 1911, we assess whether carbonate deposition would occur today if the spring orifice had been left undisturbed, in order to establish whether or not the carbonates represent conditions wetter than today. Measurements of modern spring flow rates (out of the ~3 cm diameter pipe attached to the spring box) are on the order of 0.3 L/s after dry years and 0.7 L/s after wet years (Norris and Norris, 1994). Sanders and Rott (2009) report values of 1–2 L/s and 5–10 L/s from two different sites in the Austrian Alps where *Oocardium* grows today. Comparing these Alpine values to those from Zaca suggests that despite spring capture, the flow rates emerging from the spring today are insufficiently high to sustain actively

growing *Oocardium* colonies. Furthermore, the occurrence of *Oocardium* at the distal cascade facies (Fig. 2D) implies that flow rates at the spring orifice would have had to be sufficiently high to maintain the Alpine *Oocardium* threshold rates (at least 1 L/s) throughout the extent of lateral transport (~180 m) when these waters reached the cascade. The presence of the *Oocardium* bearing tufa at the distal cascade facies thus suggests a significantly wetter climate regime during its deposition.

5.3 Oxygen Isotope Thermometry

We utilize the Hays and Grossman (1991) oxygen isotope paleotemperature equation: $T^{\circ}\text{C} = 15.7 - 4.36(\delta^{18}\text{O}_{\text{calcite}} - \delta^{18}\text{O}_{\text{water}}) + 0.12(\delta^{18}\text{O}_{\text{calcite}} - \delta^{18}\text{O}_{\text{water}})^2$ and compare values to temperature estimates derived using the Kim and O'Neil (1997) equation re-expressed by Leng and Marshall (2004) as: $T^{\circ}\text{C} = 13.8 - 4.58(\delta^{18}\text{O}_{\text{calcite}} - \delta^{18}\text{O}_{\text{water}}) + 0.08(\delta^{18}\text{O}_{\text{calcite}} - \delta^{18}\text{O}_{\text{water}})^2$ to obtain a range of depositional temperature estimates (Table 1). These equations were derived for calcite (see review in Grossman, 2012) and are thus applicable to our study, as calcite was determined to be the sole mineralogy. Both of these equations are frequently applied to freshwater carbonates (Garnett et al., 2004; Makhnach et al., 2004; Pentecost, 2005; Andrews, 2006). Differences in temperature estimates between these two equations are empirical, where temperature estimates utilizing the Hays and Grossman (1991) equation, yield warmer temperatures than the Kim and O'Neil (1997) equation (+1.8° and +3.3 °C at 25° and 0° respectively) (Grossman, 2012).

Key assumptions inherent in these temperature calculations are that (1) the carbonate precipitated in isotopic equilibrium with the spring water; (2) the water temperature during deposition as well as (3) the isotopic composition of spring water were not substantially different from today during carbonate formation. We now explore to what extent these assumptions were

problematic. For carbonate precipitation that occurs near the spring orifice, assumption (1) is often incorrect as rapid degassing might cause carbonates to precipitate before the spring water equilibrates to local atmospheric conditions (Turi, 1986). In this study, carbonates from the fluvial deposit were collected starting at about sixty meters from the spring box potentially reducing the effects of disequilibrium precipitation. Assessing assumption (2), modern water temperature has been measured twice by inserting a thermometer into the pipe downstream from the box at 14 °C and 13 °C, indicating stable spring water temperatures in a shaded riparian corridor during different seasons. Since temperatures in sub-tropical regions are thought to have not fluctuated by more than 1–2 °C over glacial-interglacial timescales (MARGO, 2009), then this temperature estimate appears to be a reasonable assumption for the past. Assumption (3) is that the *mean* $\delta^{18}\text{O}$ of modern spring water approximates that of past spring water (Table 2). If the carbonates formed from water with a similar $\delta^{18}\text{O}$ to that of today, with carbonate precipitation at or near isotopic equilibrium, then the paleotemperature estimates (Table 1) are similar to modern –in this scenario there was minimal change in either temperature or precipitation isotopes. However, if the carbonates formed during the last glacial it is possible that the spring water isotopic composition was more depleted than today. As an upper limit on how much more depleted we take the $\sim 1.5\%$ depletion in mean glacial versus Holocene $\delta^{18}\text{O}$ values of calcite from Moaning Cave in the Sierra Nevada Mountains of California (Oster et al., 2009), which is likely to see a larger shift because of its more inland and elevated location. If the $\delta^{18}\text{O}$ of spring water was 1‰ more depleted at the time of formation then this would suggest temperatures of 9.9 ± 1.0 °C (using the equation of Hays and Grossman, 1991) and 7.6 ± 1.1 °C (using the equation of Kim and O’Neil, 1997), which appear to be too cold to be reasonable given the limited expected range of sub-tropical, coastal terrestrial temperature changes. Thus

we conclude that a scenario of minimal change in the $\delta^{18}\text{O}$ values of spring water and temperature is most likely.

The mean temperature estimate using the Hays and Grossman (1991) equation is 14.1 ± 1.1 °C and 12.1 ± 1.1 °C using the Kim and O'Neil (1997) equation (Table 1). Irrespective of these modest differences between the two equations, modern temperature observations (14 °C and 13 °C) are within the calculated ranges from each equation (Fig. 7). Overall, the calculated temperatures correspond to spring water temperatures normally associated with non-thermal waters (Pentecost, 2005; Cepezzuoli et al., *Accepted article*), suggesting that the carbonates formed from ambient temperature. However, it is important to note that deposits sourced from cooled, deeply cycled (geothermal) waters have been previously described (e.g., Zhang et al., 2012), highlighting the importance of integrating textural and geochemical data to deposits of unknown affinity. Here, ambient temperature estimates (Table 1) along with the presence of *Oocardium* discredit the possibility of geothermal influence. Furthermore, the similarity of the $\delta^{18}\text{O}$ of the carbonate compared to modern water $\delta^{18}\text{O}$ (Table 2), strongly suggests the carbonate precipitated from groundwater recharged from meteoric waters, under temperatures and source water isotopic compositions relatively similar to modern. The observed variability in $\delta^{18}\text{O}$ of the carbonate within the deposits is more likely due to changes in water temperature than to source water isotopic changes given the residence time in the groundwater is expected to even out such variability.

Temperature estimates for the LBB are lower on average compared to the DBB (Fig. 7), possibly indicating that water temperature is a controlling factor on the development of *Oocardium*. However, other factors like flow rates, nutrients, water turbulence etc., might also play a significant role on the development of *Oocardium*, supported by the observation that

although common, the *Oocardium* fabric is not the only crystal fabric type (Fig. 3). Several studies of cold-water carbonates have demonstrated the potential for annual or seasonal banding, offering the possibility for very high-resolution paleoenvironmental analyses (Matsuoka et al., 2001; Kano et al., 2004; Andrews and Brasier, 2005). Bands associated with active *Oocardium* deposition have also been shown to be seasonal (Sanders and Rott, 2009), where *Oocardium* growth rates were greatest in the spring and summer. Presently, >80% of precipitation in Santa Barbara occurs in the winter (Cayan and Rhoads, 1984) suggesting that deposition may only have occurred in the winter and that $\delta^{18}\text{O}$ of winter rainfall would be a key parameter controlling the $\delta^{18}\text{O}$ of calcite.

5.4 Carbon Isotopes

Most analyses of ancient spring-associated carbonates utilize stable isotope analyses to determine the origin of the source waters (Andrews, 2006). Our carbon isotope values are strongly indicative of soil-derived CO_2 with an overall $\delta^{13}\text{C}$ range of -9.92 to -7.01‰ . The wide range in $\delta^{13}\text{C}$ and a narrower range in $\delta^{18}\text{O}$ is commonly reported in other fluvial carbonate systems (e.g., Chafetz et al., 1991). Low covariance between $\delta^{13}\text{C}$ and $\delta^{18}\text{O}$ (Fig. 8A) may be attributed to a low residence time of water in the aquifer resulting in minimal evaporation as is indicated by only a slight enrichment of $\delta^{18}\text{O}$ modern spring values compared to local precipitation and relative to the global meteoric water line (Feakins et al., 2014). Such a low degree of covariance is typical of hydrologically open systems and in this case, the $\delta^{18}\text{O}$ composition reflects local meteoric inflow (Feakins et al., 2014). Considered together, the $\delta^{13}\text{C}$ and $\delta^{18}\text{O}$ of the carbonate along with the estimated depositional temperatures shown in Table 1, present strong support for meteoric recharge of the groundwater aquifer resulting in spring water that did not undergo significant evaporation.

Given the intimate association of *Oocardium* with calcite deposition, we plot $\delta^{13}\text{C}$ values of light brown bands versus the dark brown bands in order to investigate the potential for biological photosynthetic fractionation of the resulting $\delta^{13}\text{C}$ (Fig. 8B). Our results reveal a significant $\delta^{13}\text{C}$ enrichment ($t = 2.86, p < 0.05$) in the *Oocardium* fabric compared to the dark brown bands. To date, the degree to which microorganisms can impart a photosynthetic effect on $\delta^{13}\text{C}$ of calcite via preferential uptake of $^{12}\text{CO}_2$ remains to be resolved, as it is usually complicated by the wide range of factors that may control the $\delta^{13}\text{C}$ value of calcite (Andrews, 2006). Some studies have shown a potential for biological fractionation of $^{13}\text{C}/^{12}\text{C}$ relative to bulk calcite involving cyanobacteria and some algae (Pentecost and Spiro, 1990; Arp et al., 2001), while others have shown that this discrimination is not always detectable in the calcite $\delta^{13}\text{C}$ (Shiriashi et al., 2008). Garnett et al., (2004) found that differences in $\delta^{13}\text{C}$ could be related to seasonality where during wet seasons $\delta^{13}\text{C}$ reflects relatively lighter values derived from ‘light’ soil zone carbon whereas during drier seasons the $\delta^{13}\text{C}$ contains a stronger relatively ‘heavy’ bedrock signature. However, the relatively enriched $\delta^{13}\text{C}$ values we observe correspond to *Oocardium* calcite whose depositional conditions are dependent upon high flow/moisture, thereby instead providing potential support for photosynthetic fractionation rather than bedrock/soil zone differences. The present study is the first to report calcite C and O stable isotope values associated with *Oocardium* deposition, but future work specifically on actively growing colonies of *Oocardium* is required to better constrain and assess biotic fractionation associated *Oocardium* calcite formation.

To investigate any lateral variability across facies, we plot the carbonate $\delta^{18}\text{O}$ and $\delta^{13}\text{C}$ against the distance downstream from the modern boxed spring (Fig. 9). Assuming all of the water supplying carbonate growth once originated from waters similar to the boxed spring site,

we might expect a slight increase in depositional temperature downstream and/or an overall enrichment of isotopic values resulting from progressive evaporation and CO₂ degassing (Turi, 1986; Pentecost and Spiro, 1990; Matsuoka et al., 2001). However, our data do not appear to record a pattern of (1) enrichments of $\delta^{18}\text{O}$ or $\delta^{13}\text{C}$ and thereby (2) enrichments in calculated temperature with progressive distance from the modern spring orifice (Fig. 9). Thus, it is possible that there is slight temperature variability each time each facies formed or that certain facies experienced more/less evaporation. Additionally, variables like changing flow rates and flow paths during deposition of different facies, changes in relative soil/plant/biologic contribution, and the potential for additional underground water recharge downstream may cause the stable isotope values to lack a facies trend with distance from the spring orifice (Arenas-Abad et al., 2010).

5.5 Significance for climate studies in southern California

We have established that inactive spring carbonates near Zaca Lake in Santa Barbara California were sourced from ambient temperature water with a strong soil zone $\delta^{13}\text{C}$ signal (Table 1). The presence of *Oocardium* constrains its associated depositional environment including spring flow, temperature, and humidity. Based on studies of European tufa, Pentecost (1995) noted that tufa deposits in general occur in areas characterized by average annual temperatures ranging between 5–15° C and annual rainfall exceeding 500 mm, although tufas from semi-arid environments have been described. Tufa sites with active *Oocardium stratum*, however, are more commonly found where rainfall exceeds 1,000 mm per year. Modern tufa sites reported in Montgomery County Virginia and the Arbuckle Mountains Oklahoma both contain extensive *Oocardium stratum* growth and both of these sites experience more than 1,000 mm of rainfall a year. Additionally, a study by Gradzinski (2010) documented the growth rates

of four active tufa deposits of Poland and Slovakia. *Oocardium* growth was only observed at the site that experiences greater than 1,000 mm of rainfall per year, which suggests that perhaps an ample water supply is also a controlling factor on *Oocardium* growth.

Zaca Lake currently experiences an average winter temperature of 9 °C and an average annual precipitation of ~740 mm (PRISM data, 1895-2011; Daly et al., 2008), with high inter-annual variability and over 80% of the rainfall occurring between October and March. The presence of this carbonate deposit and the occurrence of *Oocardium stratum* constitute compelling evidence for much wetter conditions in this region during carbonate formation. Of particular importance is the occurrence of the perched deposit (presently ~10 m above the boxed spring site) indicating a time of deposition for the perched cascade when the water table was significantly higher, possibly early Holocene or the Last Glacial Maximum.

6. Conclusions

This study explores the carbonate fabrics and associated stable carbon and oxygen isotopic composition of currently-inactive spring carbonate deposits near Zaca Lake in Southern California. Stable isotopic analyses of carbonate $\delta^{18}\text{O}$ are consistent with deposition in ambient temperature water (~11–16 °C). A mean $\delta^{13}\text{C}$ value of $-9.00 \pm 0.62 \text{‰}$ (1σ , $n=27$), is characteristic of soil derived CO_2 . The discovery of the calcite microstructure of the unusual desmid *Oocardium stratum* across all facies surveyed provides complimentary support to the stable isotopic data indicating that this is a tufa (ambient) rather than a travertine (hot spring) deposit, highlighting the utility of the *Oocardium* calcite microstructure as an indicator of depositional water temperature and flow conditions in ancient/inactive deposits. The presence of cold-water spring carbonates influenced by groundwater input has potential to record past

pluvials. We conclude that the carbonates grew at some time in the recent past when conditions were wetter.

7. Acknowledgements

We thank the Zaca Lake Retreat Staff for access to Zaca Lake. We thank A. Lopez, K. Zacny, G. Paulsen, and L. Beegle and for field assistance and Miguel Rincon for isotopic analyses of carbonates. M. Kirby, S. Lund, and W. Berelson provided insightful discussions throughout this project. This manuscript was improved by the comments of Editor Brian Jones, and reviewers Michal Gradzinski and Mike Rogerson and other anonymous reviewers. This research was supported by the Geological Society of America graduate student research grant to YI, US National Science Foundation Grant EAR-1002656 to S.F and US National Aeronautics and Space Agency award to F.C.

References

- Anderson, T.F., Arthur, M.A., 1983. Stable isotopes of oxygen and carbon and their application to sedimentological and palaeoenvironmental problems. In: Arthur, M.A. Anderson, T.F. Kaplan, I.R. Veizer, J., Land, L.S., (Eds.), *Stable Isotopes in Sedimentary Geochemistry*: Society of Economic Palaeontologists and Mineralogists Short course 10, pp 1.1–1–151.
- Andrews, J.E., 2006. Palaeoclimatic records from stable isotopes in riverine tufas: Synthesis and review. *Earth Science Reviews* 75, 85–104.
- Andrews, J.E., Brasier, A.T., 2005. Seasonal records of climatic change in annually laminated tufas: short review and future prospects. *Journal of Quaternary Science* 20, 411–421.
- Arenas-Abad, C., Vazquez-Urbez, M., Pardo-Tirapu, G., Sancho-Marcen, C., 2010. Fluvial and associated carbonate deposits. In: Alonso-Zarza, A.M, Tanner, L.H. (Eds.), *Carbonates*

- in Continental Settings: Facies, Environments and Processes. *Developments in Sedimentology* 61, 133–175.
- Arp, G., Wedemeyer, N., Reitner, J., 2001, Fluvial tufa formation in a hard-water creek (Deinschwanger Bach, Franconian Alb, Germany). *Facies* 44, 1–622.
- Arp, G., Bissett, A., Brinkmann, N., Cousin, S., Beer, D.D., Friedl, T., Mohr, K.I., Neu, T.R., Reimer, A., Shiraishi, F., Stackebrandt, E., Zippel, B., 2010. Tufa-forming biofilms of German karstwater streams: microorganisms, exopolymers, hydrochemistry and calcification. Geological Society, London, Special Publications 336, 83–118.
- Cayan, D.R., Rhoads, J., 1984. Local relationships between United States west coast precipitation and monthly mean circulation parameters. *Monthly Weather Review* 112, 1276–1282.
- Capezzuoli, E., Gandin, A., Sandrelli, F., 2008. Evidence of associated deposition of travertine and calcareous tufa in the Quaternary carbonates of Valdelsa Basin (Tuscany). *Italian Journal of Quaternary Sciences* 21, 113–124.
- Capezzuoli, E., Gandin, A., Pedley, M., *Accepted article*. Decoding tufa and travertine (fresh water carbonates) in the sedimentary record: The state of the art. *Sedimentology* doi: 10.1111/sed.12075.
- Chafetz, H.S., Utech, N.M., Fitzmaurice, S.P., 1991. Differences in the $\delta^{18}\text{O}$ and $\delta^{13}\text{C}$ signatures of seasonal laminae comprising travertine stromatolites. *Journal of Sedimentary Petrology* 61, 1015–1028.
- Crevaschi, M., Zerboni, A., Spötl, C. and Felletti, F., 2010. The calcareous tufa in the Tadrart Acacus Mt. (SW Fezzan, Libya) An early Holocene palaeoclimate archive in the central Sahara. *Palaeogeography, Palaeoclimatology, Palaeoecology* 287, 81–94.

- Daly, C., Halbleib, M., Smith, J.I., Gibson, W.P., Doggett, M.K., Taylor, G.H., Curtis, J., Pasteris, P.P., 2008. Physiographically sensitive mapping of climatological temperature and precipitation across the conterminous United States. *International Journal of Climatology* 28, 2031–2064.
- Dansgaard, W., 1964. Stable isotopes in precipitation. *Telus* 16, 436–468.
- Feakins, S.J., Kirby, M.E., Cheetham, M.I., Ibarra, Y., Zimmerman, S.R., 2014. Fluctuation in leaf wax D/H ratio from a southern California lake records significant variability in isotopes in precipitation during the late Holocene. *Organic Geochemistry* 66, 48–59.
- Ford, T.D., Pedley, H.M., 1996. A review of tufa and travertine deposits of the world. *Earth Science Reviews* 41, 117–175.
- Fouke, B.W., Farmer, J.D., Des Marais, D.J., Pratt, L., Sturchio, N.C., Burns, P.C., Discipulo, M.K., 2000. Depositional facies and aqueous-solid geochemistry of travertine-depositing hot springs (Angel Terrace, Mammoth Hot Springs, Yellowstone National Park, U.S.A.). *Journal of Sedimentary Research* 70, 565–585.
- Freytet, P., Plet, A., 1996. Modern Freshwater Microbial Carbonates: The Phormidium Stromatolites (Tufa-Travertine) of Southeastern Burgundy (Paris Basin, France). *Facies* 34, 219–237.
- Freytet, P., Verrecchia, E.P., 1998. Freshwater organisms that build stromatolites: a synopsis of biocrystallization by prokaryotic and eukaryotic algae. *Sedimentology* 45, 535–563.
- Gandin, A., Capezzuoli, E., 2008. Travertine versus calcareous tufa: Distinctive petrologic features and stable isotopes signatures. *Italian Journal of Quaternary Sciences* 21, 125–136.
- Garnett, E.R., Andrews, J.E., Preece, R.C., Dennis, P.F., 2004. Climatic change recorded by

- stable isotopes and trace elements in a British Holocene tufa. *Journal of Quaternary Science* 19, 251–262.
- Gesierich, D., Kofler, W., 2010. Are algal communities from near-natural rheocene springs in the Eastern Alps (Vorarlberg, Austria) useful ecological indicators? *Algological Studies* 133, 1–28.
- Golubić, S., Violante, C. and Ferreri, V., 1993. Algal control and early diagenesis in Quaternary travertine formation (Rocchetta a Volturno, Central Apennines). In: F. Baratolo, P. De Castro and M. Parente (Editors), *Studies on fossil benthic algae*. *Boll. Soc. Paleontol. Ital*, pp. 231–247.
- Golubić, S., Violante, C., Plenković-Moraj, A., Grgasović, T., 2008. Travertines and calcareous tufa deposits: an insight into diagenesis. *Geologia Croatica* 61, 363–378.
- Gonfiantini, R., Panichi, C. and Tongiorgi, E., 1968. Isotopic disequilibrium in travertine deposition. *Earth and Planetary Science Letters* 5, 55–58.
- Grossman, E.L., 2012. Applying oxygen isotope thermometry in deep time. In: L.C. Ivany, and B.T. Huber (Editors), *Reconstructing Earth's deep time climate—The state of the art in 2012*, Paleontological Society Short Course, pp. 39–67.
- Gradzinski, M., 2010. Factors controlling growth of modern tufa: results of a field experiment. Geological Society, London, Special Publications 336, 143–191.
- Guo, L., Andrews, J., Riding, R., Dennis, P. and Dresser, Q., 1996. Possible microbial effects on stable carbon isotopes in hot-spring travertines. *Journal of Sedimentary Research* 66, 468–473.
- Hall, C.A., 1981. Map of geology along the Little Pine Fault, parts of the Sisquoc, Foxen Canyon, Zaca Lake, Bald Mountain, Los Olivos, and Figueroa Mountain quadrangles,

- Santa Barbara County, California, Miscellaneous Field Studies Map MF-1285 scale, 1:24000. U.S. Geological Survey.
- Hancock, P.L., Chalmers, R.M.L., Altunel, E. and Çakir, Z., 1999. Travitronics: using travertines in active fault studies. *Journal of Structural Geology* 21, 903–916.
- Hays, P.D., Grossman E.L., 1991. Oxygen isotopes in meteoric calcite cements as indicators of continental paleoclimate. *Geology* 19, 441–444.
- Kano, A., Kawai, T., Matsuoka, J., Ihara, T., 2004. High-resolution records of rainfall events from clay bands in tufa. *Geology* 32, 793–796.
- Kele, S., Demény, A., Siklósy, Z., Németh, T., Tóth, M., Kovács, M.B., 2008. Chemical and stable isotope composition of recent hot-water travertines and associated thermal waters, from Egerszalok, Hungary: Depositional facies and non-equilibrium fractionation. *Sedimentary Geology* 211, 53–72.
- Kim, S.T., O’Neil, J.R., 1997. Equilibrium and nonequilibrium oxygen isotope effects in synthetic carbonates. *Geochimica et Cosmochimica Acta* 61, 3461–3475.
- Leng, M.J., Marshall, J. D., 2004. Palaeoclimate interpretation of stable isotope data from lake sediment archives. *Quaternary Science Reviews* 23, 811–831.
- Linhart, C., 2011. Autecology of *O. stratum* and algae associated travertine precipitation: deposition rate and algal community composition DeLi Seminar Program Summer 2011, University of Vienna.
- Makhnach, N., Zernitskaja, V., Kolosov, I., Simakova, G., 2004. Stable oxygen and carbon isotopes in Late Glacial-Holocene freshwater carbonates from Belarus and their palaeoclimatic implications. *Palaeogeography, Palaeoclimatology, Palaeoecology* 209, 73–101.

- Manzo, E., Perri, E., Tucker, M.E., 2012. Carbonate deposition in a fluvial tufa system: processes and products (Corvino Valley – Southern Italy). *Sedimentology* 59, 553–577.
- MARGO, 2009. Constraints on the magnitude and patterns of ocean cooling at the Last Glacial Maximum. *Nature Geoscience* 2, 127–132.
- Mathews, H.L., Prescott, G.W., Obenshain, S.S., 1965. The genesis of certain calcareous floodplain soils of Virginia. *Soil Science Society of America Journal* 29, 729–732.
- Matsuoka, J., Kano, A., Oba, T., Watanabe, T., Sakai, S., Seto, K., 2001. Seasonal variation of stable isotopic compositions recorded in a laminated tufa, SW Japan. *Earth and Planetary Science Letters* 192, 31–44.
- Minissale, A., Kerrick, D.M., Magro, G., Murrell, M.T., Paladini, M., Rihs, S., Sturchio, N.C., Tassi, F., Vaselli, O., 2002. Geochemistry of Quaternary travertines in the region north of Rome (Italy): structural, hydrologic and paleoclimatic implications. *Earth and Planetary Science Letters* 203, 709–728.
- Oster, J.L., Montañez, I.P., Sharp, W.D., Cooper, K. M., 2009. Late Pleistocene California droughts during deglaciation and Arctic warming. *Earth and Planetary Science Letters* 288, 434–443.
- Nägeli, C., 1849. *Gattungen einzelliger Algen*. Friedrich Schulthess, Zürich: 74–76.
- Norris J., Norris, L., 1994. *History of Zaca Lake*, Olive Press Publications, Los Olivos, CA, 191 pp.
- Pedley, H.M., 1990. Classification and environmental models of cool freshwater tufas. *Sedimentary Geology* 68, 143–154.
- Pedley, H.M., 2009. Tufas and travertines of the Mediterranean region: a testing ground for

- freshwater carbonate concepts and developments. *Sedimentology* 56, 221–246.
- Pentecost, A., 1990. The algal-flora of travertine: An overview. *Travertine marl; stream deposits in Virginia* 101, 117–128.
- Pentecost, A., 1991. A new and interesting site for the Calcite-encrusted desmid *Oocardium stratum* Naeg. in the British Isles. *European Journal of Phycology* 26, 297–301.
- Pentecost, A., 1995. The Quaternary travertine deposits of Europe and Asia Minor. *Quaternary Science Reviews* 14, 1005–1028.
- Pentecost, A., 2005. *Travertine*. Springer, Berlin, 460 pp.
- Pentecost, A., Spiro, B., 1990. Stable carbon and oxygen isotope composition of calcites associated with modern freshwater cyanobacteria and algae. *Geomicrobiology Journal* 8, 17–26.
- Pentecost, A., Zhang, Z., 2000. The travertine flora of Juizhaigou and Munigou, China, and its relationship with calcium carbonate deposition. *Cave and Karst Science* 27, 71–78.
- Pfiester, L.A., 1976. *Oocardium stratum* A rare (?) Desmid (Chlorophyceae). *Journal of Phycology* 12, 134.
- Riding, R., 2000. Microbial carbonates: the geological record of calcified bacterial-algal mats and biofilms. *Sedimentology* 47, 179–214.
- Rott, E., Holzinger, A., Gesierich, D., Kofler, W., Sanders, D., 2009. Cell morphology, ultrastructure, and calcification pattern of *Oocardium stratum*, a peculiar lotic desmid. *Protoplasma* 243, 39–50.
- Sanders, D., Rott, E., 2009. Contrasting styles of calcification by the micro-alga *Oocardium stratum* Naegeli 1849 (Zygnematophyceae) in two limestone-precipitating spring creeks of the Alps. *Austrian Journal of Earth Sciences* 102, 34–49.

- Sanders, D., Wertl, W., Rott, E., 2011. Spring-associated limestones of the Eastern Alps: overview of facies, deposystems, minerals, and biota. *Facies* 57, 395–416.
- Shapiro, R.S., 2000. A comment on the systematic confusion of thrombolites. *Palaios* 15, 166–169.
- Szulc, J., Cwizewicz, M., 1989. The Lower Permian freshwater carbonates of the Slawkow Graben, Southern Poland: sedimentary facies context and isotope study. *Palaeogeography, Palaeoclimatology, Palaeoecology* 70, 107–120.
- Turi, B., 1986. Stable isotope geochemistry of travertines. In: Fritz, B.P., Fontes, J.C. (Eds.), *Handbook of Environmental Isotope Geochemistry*. Elsevier, Amsterdam, pp. 207–238.
- United States Geological Survey, 1995. Zaca Lake Quadrangle (Topographic Map). 1:24,000. 7.5 Minute Series, Washington D.C.
- Viles, H.A., Taylor, M.P., Nicoll, K., Neumann, S., 2007. Facies evidence of hydroclimatic regime shifts in tufa depositional sequences from the arid Naukluft Mountains, Namibia. *Sedimentary Geology* 195, 39–53.
- Wallner, J., 1933. *Oocardium stratum* Naeg., eine wichtige tuffbildende Alge Südbayerns. *Planta* 20, 287–293.
- Zhang, J., Wang, H., Liu, Z., An, D., Dreybrodt, W., 2012. Spatial-temporal variations of travertine deposition rates and their controlling factors in Huanglong Ravine, China- A world's heritage site. *Applied Geochemistry* 27, 211–222.

Fig. 1. Geologic setting of the spring carbonates. (A) Geologic map of the Zaca Lake catchment. Abbreviations: M=Monterey; Qs=surface Quaternary; L=landslide; Tv= Tertiary volcanics. Dashed lines indicate fault lines. Contours are at 200 m intervals. (B) Schematic representation

of carbonate deposit (imitating Viles et al., 2007) with the labeled location of the boxed spring, fluvial deposit, and spring deposit (the image is not drawn to scale; the approximate distance from the boxed spring to the cascade is ~180 m).

Fig. 2. Facies of the spring carbonate deposits. (A) Cascade facies of the perched deposit displaying overhanging carbonate curtains. (B) Barrage deposits. (C) Fluvial channel. (D) Terminal fluvial cascade deposit with people on the outcrop for scale.

Fig. 3. Mesostructure of the spring carbonate fabrics from the four facies in Fig. 2. (A) Banded carbonate from the outermost cascade wall of the perched deposit. (B) Broken carbonate piece from the fluvial terrace channel. (C-D) Microphyte-encrusted carbonate and banded carbonate from the barrage deposits. (E) Banded carbonate from the terminal cascade facies. White arrows denote the light brown bands.

Fig. 4. Meso and microstructure of the spring carbonate fabric. (A) Freshly broken piece displaying the texture of the light brown bands (LBB). (B) Polished hand sample denoting the contrast between the dark brown bands (DBB) and LBB. (C) Photomicrograph of a light and dark couplet. (D) Well-defined calcite crystal terminations comprising the DBB (E) Calcite tubules (~20 μm in diameter) comprising the LBB.

Fig. 5. Microstructure of the light brown bands. (A) Several adjacent calcite tubule bundles. (B) Adjacent calcite tubule bundles (same as Fig. 3A) under cross-polarized light. (C) Oblique SEM image of the bottom of several tubule bundles demonstrating that each bundle originates from a common point. (D) Photomicrograph of calcite tubules. (E) SEM image of the top of several tubules displaying their hollow nature. (F) Horizontal cross section through a tubule bundle showing round voids of consistent diameter (~20 μm). (G) SEM image displaying tubule voids.

Fig. 6. Photomicrographs of the *Oocardium stratum* calcite microstructure. (A) Three distinct oblique sections of *Oocardium* colonies labeled with a “c”. (B) Several adjacent tubule bundles. (C) The bundles are composed of tubules whose growth terminates at the intersection with other fans. (D) Horizontally and vertically oriented junction of two tubule bundles, arrows denote sites that *Oocardium* cells might have once inhabited.

Fig. 7. Box and whisker plots of calculated temperature estimates comparing the light brown and dark brown bands, where the whiskers represent the range, the box represents the upper and lower quartiles and the black horizontal line within the boxes denotes the median.

Fig. 8. Carbonate stable carbon and oxygen isotope results. (A) Carbonate $\delta^{13}\text{C}$ and $\delta^{18}\text{O}$ cross plot. (B) $\delta^{13}\text{C}$ box and whisker plots (see caption of Fig. 7) of light brown bands and dark brown bands.

Fig. 9. Stable isotope plots versus distance from the boxed spring. (A) $\delta^{18}\text{O}$ versus distance from the boxed spring. (B) $\delta^{13}\text{C}$ versus distance from the boxed spring. Note: Data from the perched cascade is not included in these plots as those carbonates formed away from the boxed spring fluvial path.

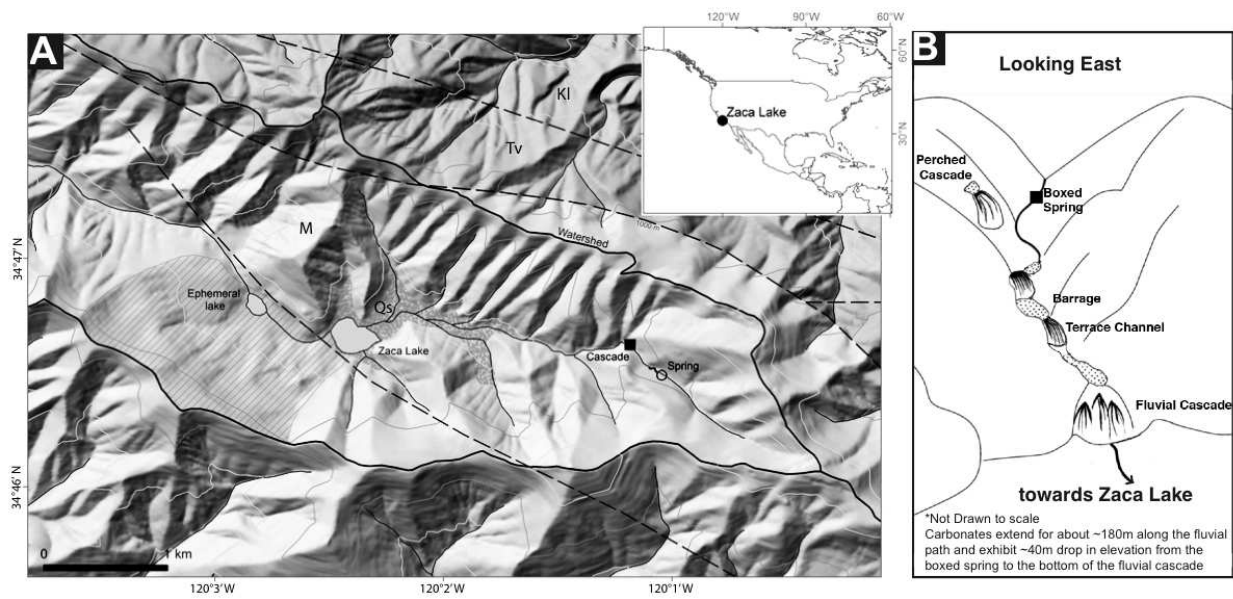


Figure 1

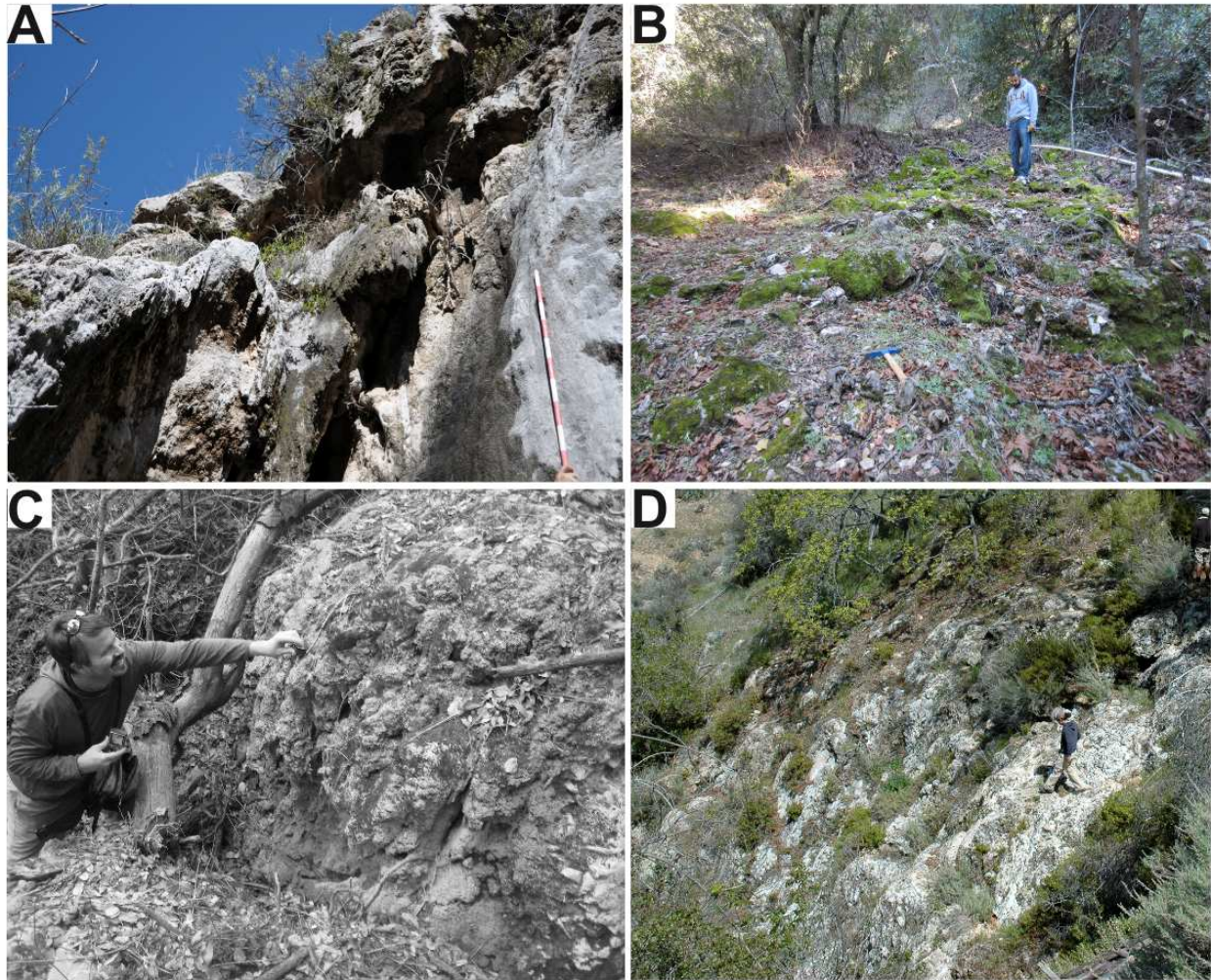


Figure 2

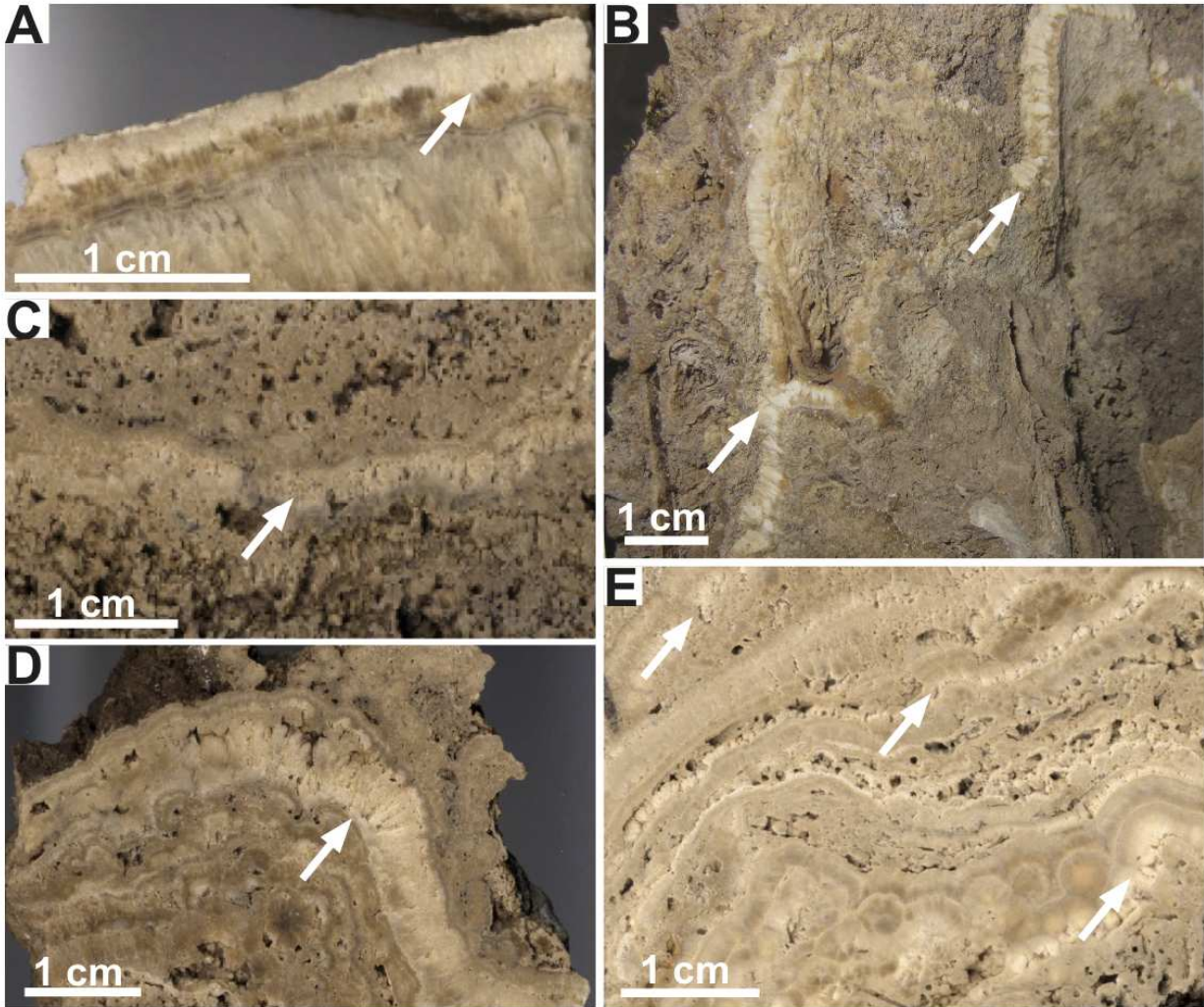


Figure 3

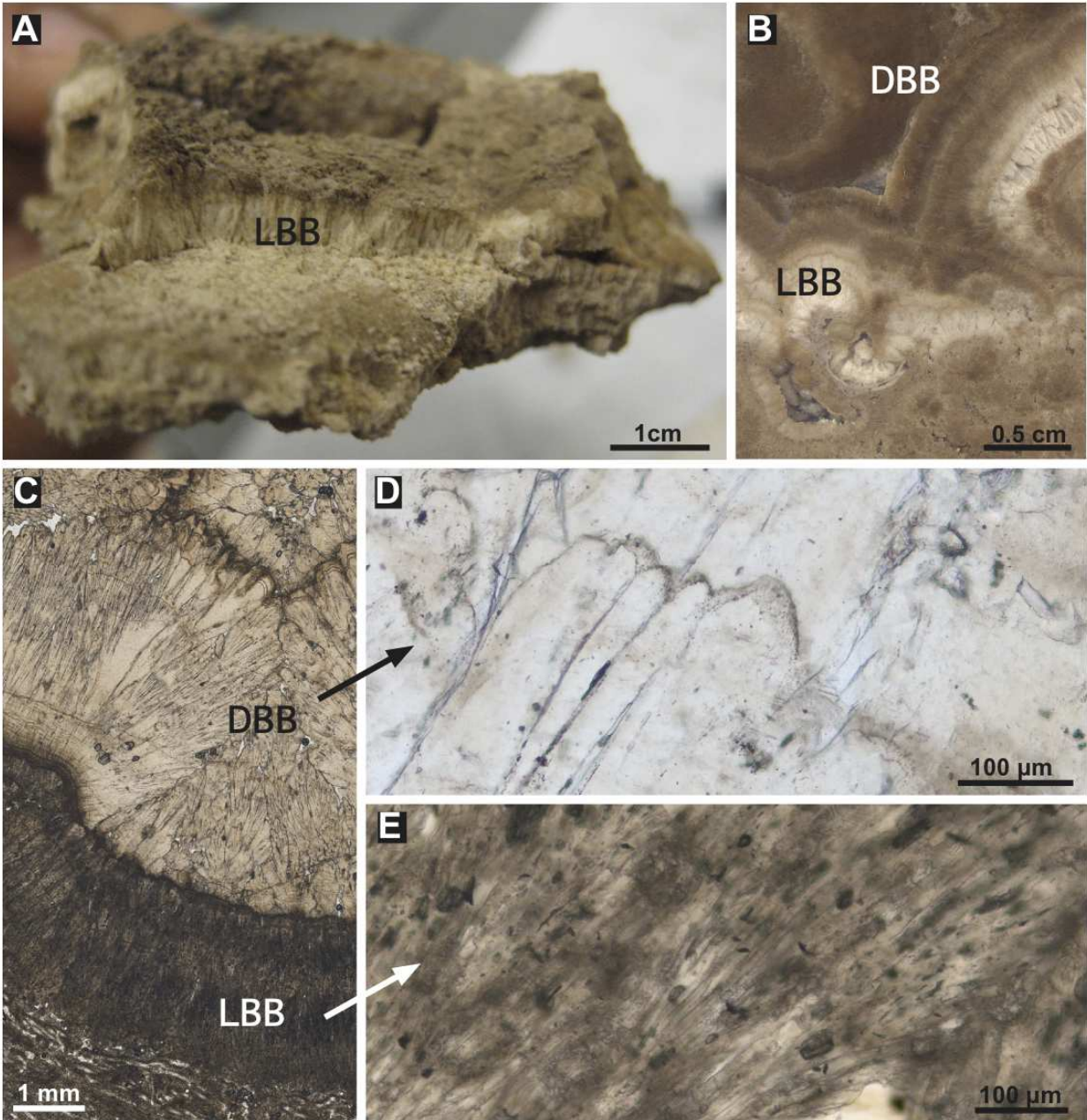


Figure 4

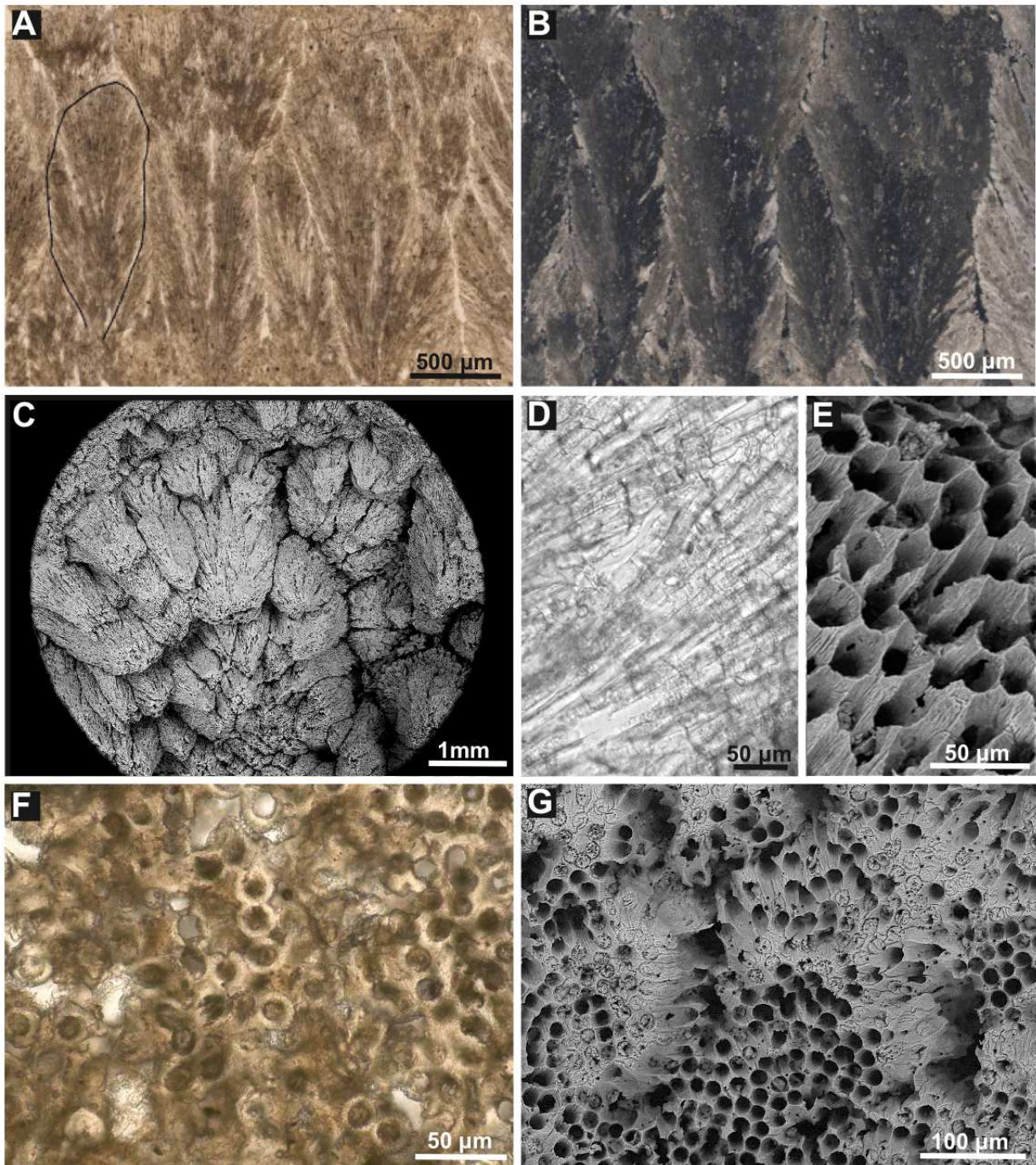


Figure 5

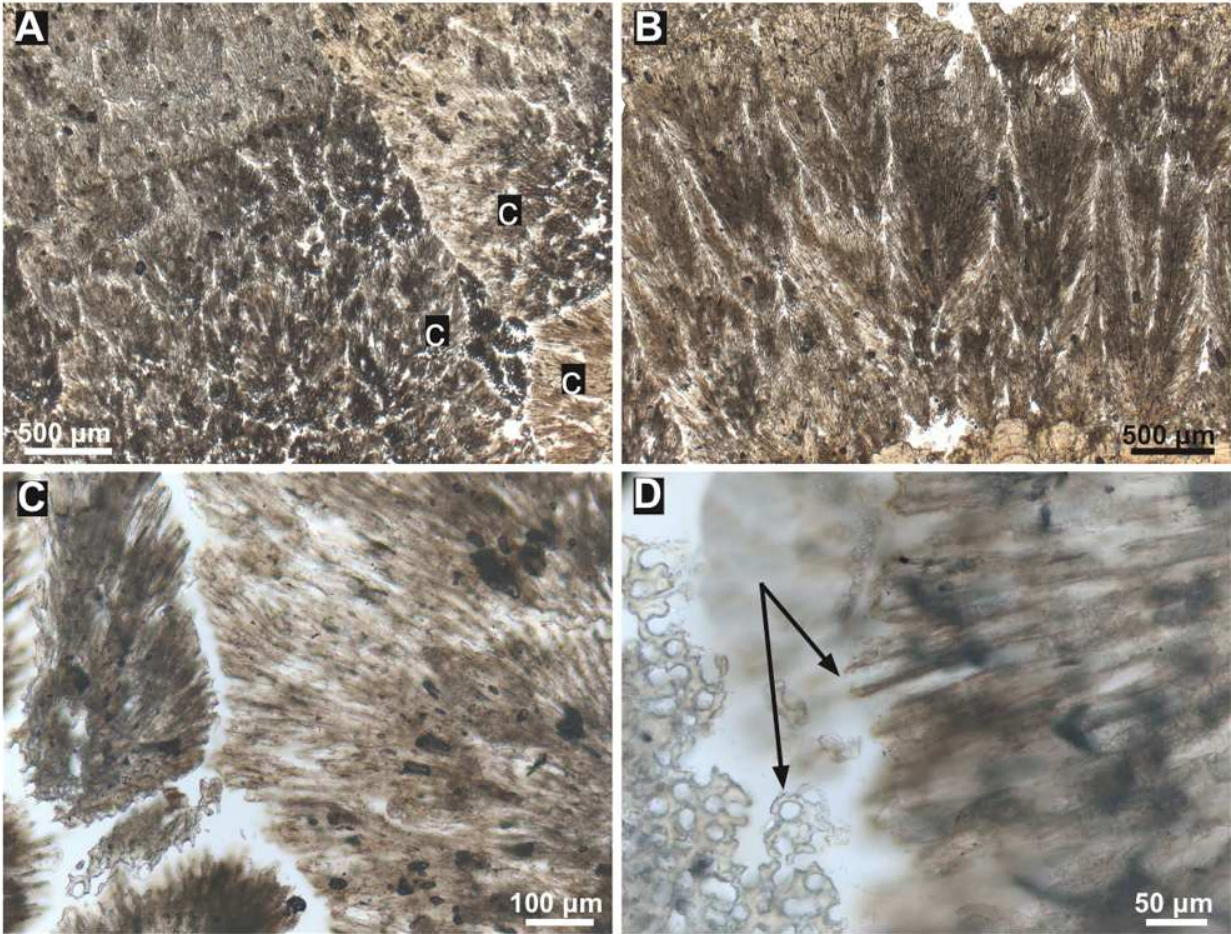


Figure 6

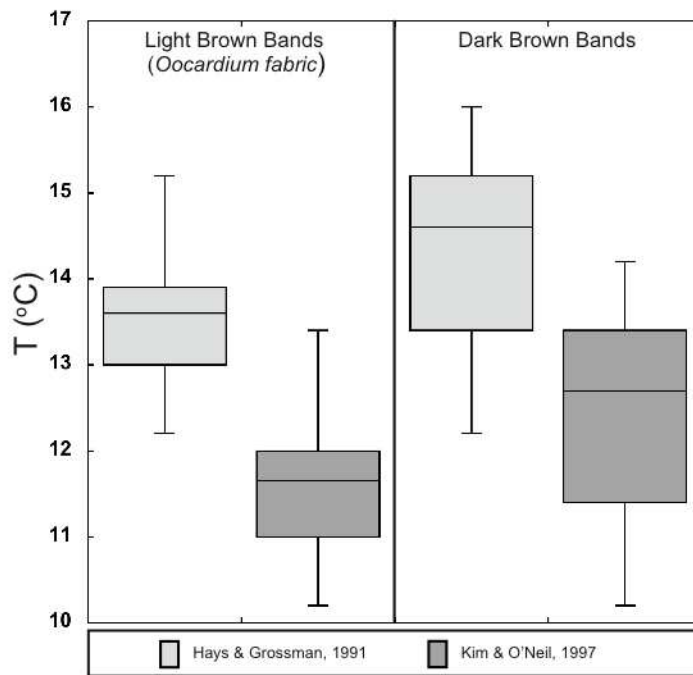


Figure 7

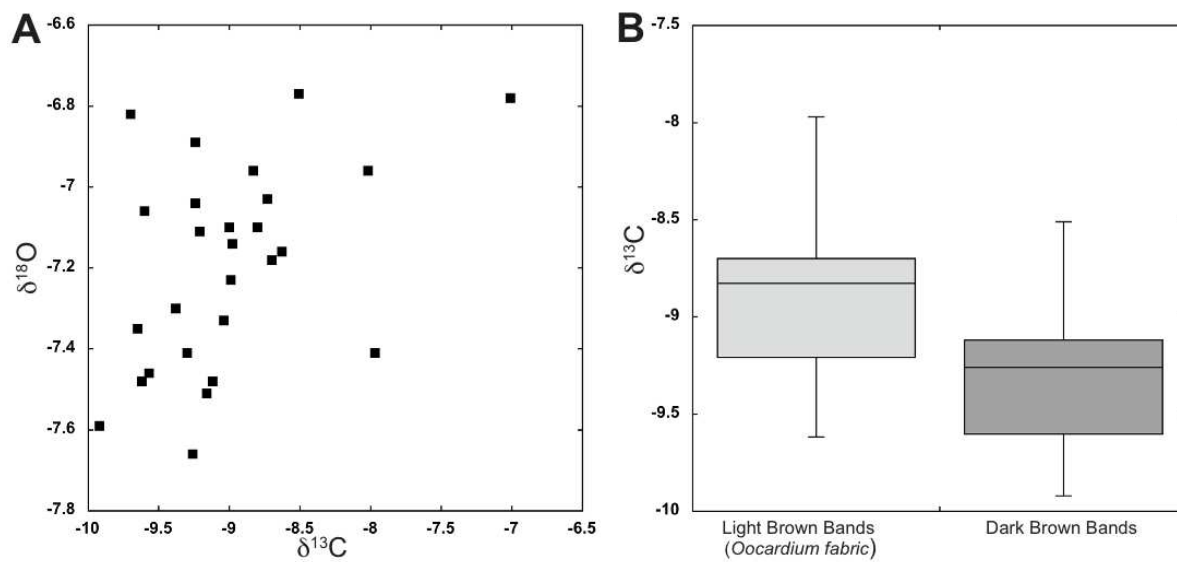


Figure 8

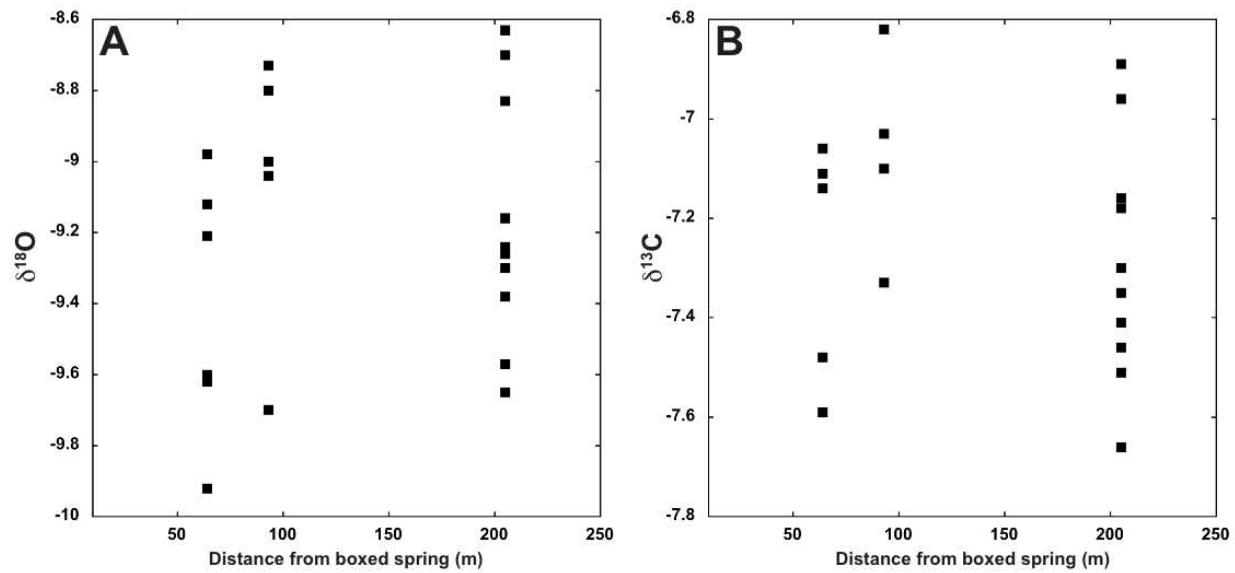


Figure 9

Table 1Stable isotopic compositions of $\delta^{18}\text{O}$ and $\delta^{13}\text{C}$ (‰ VPDB) for carbonate from their corresponding facies

Facies and Distance from boxed spring (m)	Fabric type	Sample	$\delta^{13}\text{C}_{\text{carb}}$	$\delta^{18}\text{O}_{\text{carb}}$	$\delta^{13}\text{C}_{\text{carb}}$ 1 σ (‰)	$\delta^{18}\text{O}_{\text{carb}}$ 1 σ (‰)	Calculated Temp. (°C) Hays & Grossman, 1991	Calculated Temp. (°C) Kim & O'Neil, 1997
Perched Cascade (~10m above boxed spring)	LBB	Zpc-ooc2	-7.01	-6.78			12.2	10.2
		Zpc-ooc3	-7.97	-7.41			14.9	13.0
		PC2A	-8.02	-6.96			12.9	11.0
	DBB	Zpc-d1	-8.51	-6.77			12.2	10.2
		Zpc-d2	-8.99	-7.23			14.1	12.2
		PC2d	-9.24	-7.04			13.3	11.4
Fluvial Barrage (~60)	LBB	ZPooc13*	-9.62	-7.48	0.01	0.13	15.2	13.4
		Zb-oc-b	-9.21	-7.11			13.6	11.7
		Zb-oc-t	-8.98	-7.14			13.7	11.8
	DBB	ZPd13*	-9.92	-7.59	0.13	0.19	15.7	13.9
		Zb-d	-9.12	-7.48			15.2	13.4
		Zpd4	-9.60	-7.06			13.4	11.4
Fluvial Terrace Channel (~90)	LBB	Ztooc12*	-8.80	-7.10	0.71	0.20	13.5	11.6
		Ztooc45*	-8.73	-7.03	0.20	0.08	13.3	11.3
		Ztooc6	-9.00	-7.10			13.6	11.6
	DBB	Ztd12*	-9.70	-6.82	0.21	0.01	12.4	10.4
		Ztd45*	-9.04	-7.33	0.14	0.07	14.6	12.7
		ZOC2*	-9.30	-7.41	0.53	0.03	14.9	13.0
Fluvial Cascade (~180)	LBB	OC	-9.24	-6.89			12.7	10.7
		FC-01	-8.70	-7.18			13.9	12.0
		FC-02	-8.63	-7.16			13.8	11.9
	DBB	FC03*	-8.83	-6.96	0.17	0.06	13.0	11.0
		ZA1	-9.65	-7.35			14.6	12.8
		ZM1	-9.16	-7.51			15.3	13.5
		ZA2	-9.57	-7.46			15.1	13.3
		FC-D1-1	-9.26	-7.66			16.0	14.2
		FC-D3*	-9.38	-7.30	0.22	0.06	14.4	12.5
Mean Overall			-9.01	-7.20			14.1	12.1
1σ			0.62	0.25			1.1	1.1
Mean LBB			-8.71	-7.12			13.8	11.8
Mean DBB			-9.31	-7.27			14.2	12.2

*Samples whose values represent the *mean* $\delta^{18}\text{O}$, $\delta^{13}\text{C}$, and temperature of at least three measurements along the respective sample band. LBB: light brown bands; DBB: dark brown bands

Table 2Stable isotopic compositions of $\delta^{18}\text{O}$ and δD of modern water samples from Zaca Spring

Collection Date	Water $\delta^{18}\text{O}$ (‰ VSMOW)	δD (‰ VSMOW)
14 Feb 2009	-7.30	-47.0
30 Oct 2009	-7.70	-47.0
25 Feb 2010	-7.70	-46.3
11 Jun 2010	-7.70	-47.0
5 Nov 2010	-7.70	-48.0
5 Apr 2011	-7.80	-48.0
27 Sep 2011	-7.14	-41.4
16 Apr 2012	-7.62	-48.7
<i>Mean</i>	-7.58	-46.7
<i>1σ</i>	0.23	2.3